

Magnetically Hidden State on the Ground Floor of the Magnetic Devil's Staircase

S. Imajo^{1,*}, N. Matsuyama,¹ T. Nomura¹, T. Kihara,^{2,†} S. Nakamura,² C. Marcenat³, T. Klein,⁴ G. Seyfarth⁵,
C. Zhong,^{6,‡} H. Kageyama,⁶ K. Kindo,¹ T. Momoi^{7,8} and Y. Kohama¹

¹*Institute for Solid State Physics, University of Tokyo, Kashiwa, Chiba 277-8581, Japan*

²*Institute for Materials Research, Tohoku University, Sendai 980-8577, Japan*

³*Université Grenoble Alpes, CEA, Grenoble INP, IRIG, PHELIQS, 38000 Grenoble, France*

⁴*Université Grenoble Alpes, CNRS, Grenoble INP, Institut Néel, F-38000 Grenoble, France*

⁵*LNCMI-EMFL, CNRS, Université Grenoble Alpes, INSA-T, UPS, F-38042 Grenoble, France*

⁶*Graduate School of Engineering, Kyoto University, Kyoto 615-8510, Japan*

⁷*Condensed Matter Theory Laboratory, RIKEN, Wako, Saitama 351-0198, Japan*

⁸*RIKEN Center for Emergent Matter Science (CEMS), Wako, Saitama 351-0198, Japan*

 (Received 14 March 2022; revised 20 June 2022; accepted 8 September 2022; published 29 September 2022)

We investigated the low-temperature and high-field thermodynamic and ultrasonic properties of $\text{SrCu}_2(\text{BO}_3)_2$, which exhibits various plateaux in its magnetization curve above 27 T, called a magnetic Devil's staircase. The results of the present study confirm that magnetic crystallization, the first step of the staircase, occurs above 27 T as a first-order transition accompanied by a sharp singularity in heat capacity C_p and a kink in the elastic constant. In addition, we observe a thermodynamic anomaly at lower fields around 26 T, which has not been previously detected by any magnetic probes. At low temperatures, this magnetically hidden state has a large entropy and does not exhibit Schottky-type gapped behavior, which suggests the existence of low-energy collective excitations. Based on our observations and theoretical predictions, we propose that magnetic quadrupoles form a spin-nematic state around 26 T as a hidden state on the ground floor of the magnetic Devil's staircase.

DOI: [10.1103/PhysRevLett.129.147201](https://doi.org/10.1103/PhysRevLett.129.147201)

The orthogonal dimer antiferromagnet $\text{SrCu}_2(\text{BO}_3)_2$ [1,2] has been intensively studied owing to its unique magnetic properties under extreme conditions, such as high pressure and high magnetic field. As shown in the inset of Fig. 1, $\text{SrCu}_2(\text{BO}_3)_2$ has a two-dimensional (2D) layered structure comprising Cu^{2+} ($S = 1/2$) with the competing antiferromagnetic interactions J and J' . This spin alignment, the so-called Shastry-Sutherland lattice, has strong geometrical frustration [3,4]. The macroscopic degeneracy arising from the geometrical frustration is lifted under extreme conditions, which results in the appearance of various quantum magnetic states. Recent studies have investigated how high pressure modifies the ratio of J'/J and the competition among the magnetic states, such as a dimer singlet, a plaquette singlet, and an antiferromagnetic order [5–10]. Meanwhile, under sufficiently strong magnetic fields, the frustration in the Shastry-Sutherland lattice leads to an intricate magnetization process including a peculiar series of plateaux [11–15], which has been called a magnetic Devil's staircase. Each magnetization plateau can be viewed as a Wigner crystal of triplets or higher multiplets, where the geometrical frustration suppresses the hopping of triplet bosons, leading to the crystallization of multiplets with a nontrivial magnetic superstructure.

While the $S^z = 1$ triplet boson plays a crucial role in the emergence of the magnetization plateau, the $S^z = 2$ bound

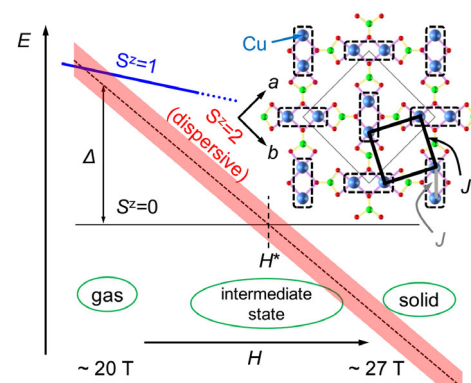


FIG. 1. Schematic illustration of a one-particle energy diagram for $S^z = 0, 1,$ and 2 levels in magnetic fields based on the ESR study [16]. At around 20 T, the $S^z = 2$ level (red band) falls below the $S^z = 1$ level (blue line). Far below (above) H^* , the state is regarded as a gas (solid) phase of the bound triplets. A possible intermediate phase between the gas and solid phases appears within the proximity of H^* . Importantly, many-body effects among multiple particles in real materials complicate this energy diagram around H^* , which should make its details unpredictable. The inset illustrates the crystal structure of $\text{SrCu}_2(\text{BO}_3)_2$ viewed along the c axis. The dashed rectangles represent dimers of the spin- $1/2$ Cu^{2+} ions. The thick black and gray lines indicate the antiferromagnetic exchange interactions J and J' , respectively.

triplet pair is critical for understanding certain plateaux. According to theoretical studies [17,18], the magnetic crystals of the $S^z = 2$ bound states are energetically more favorable than those of the $S^z = 1$ triplets for some low-field plateaux. As shown in the schematic in Fig. 1, an ESR study [16] indicates that the $S^z = 2$ level, becoming lower than the $S^z = 1$ above 20 T, seemingly becomes the ground state around H^* of 24 T. Within the first-order perturbation approach, the $S^z = 0$ and 2 levels cannot be hybridized even with the Dzyaloshinskii-Moriya (DM) interaction, and hence it is unclear whether these levels anticross around H^* . Compared to the dispersionless $S^z = 1$ (< 0.2 meV) and purely discrete $S^z = 0$ levels, the $S^z = 2$ level has a large dispersion (~ 1.5 meV) [19]. Notably, the description of the energy diagram in Fig. 1 is for a single particle. In the case of multiple particles in real compounds, the energy diagram is modified by the many-body effects, which should complicate the crossing of the energy levels around H^* . At fields far below H^* , the state is regarded as a gas phase of the thermally excited bound triplets. The number of bound triplets increases towards the crystallization field H_{crystal} ($= 27$ T), and the correlation effects among the bound triplets are enhanced. At H_{crystal} , a strong interaction results in the symmetry breaking with the solidification of the $S^z = 2$ states. In the thermodynamic phase diagram, a gas-solid phase boundary should generally be a first-order transition, where translational and rotational symmetries are broken simultaneously, and an intermediate phase, such as liquid and liquid crystals, often exists with partial symmetry breaking. This is analogous to a recent report [20] emphasizing a similarity between water and $\text{SrCu}_2(\text{BO}_3)_2$ in terms of physics near a first-order critical point. Indeed, as a potential intermediate phase, the Bose-Einstein condensate of the $S^z = 2$ bound triplets just below H_{crystal} has been predicted by several theoretical studies [17,18,21,22]. This phase is equivalent to the spin-nematic (SN) order, which is the liquid crystal of spins where rotational symmetry is broken while time-reversal symmetry is retained. A search for the SN phase should provide new insights into phase competition in quantum magnets. Nevertheless, it is challenging to detect the SN state using traditional magnetic probes, such as magnetization and NMR, because its order parameter is the spin quadrupole moment rather than the spin dipole moment. Hence, in this study, we searched for the SN phase using entropic measurement techniques which detects the entropy change caused by any spontaneous symmetry breakings.

Heat capacity (C_p) measurements were performed in pulsed and dc magnetic-field laboratories in ISSP (Kashiwa, Japan), IMR (Sendai, Japan), and LNCMI (Grenoble, France). The C_p data measured in pulsed magnetic fields were obtained by the quasiadiabatic method (abbreviated as QA) [23]. The data measured in the hybrid and resistive magnets were obtained using the dual-slope (DS) method and ac (AC) method, respectively. We

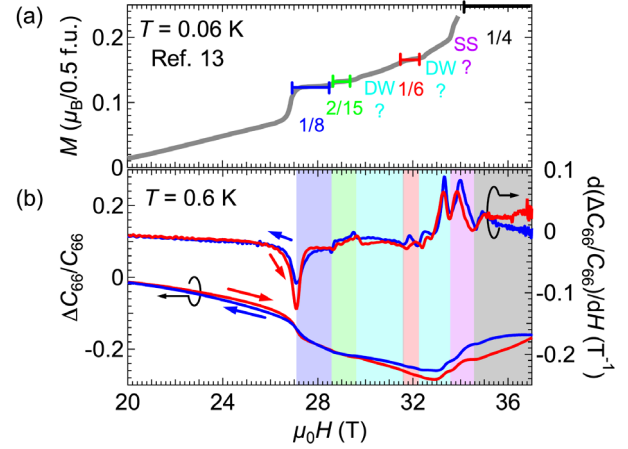


FIG. 2. (a) Low-temperature magnetization data taken from Ref. [13]. Each plateau is illustrated by the colored bars. According to the theory [17], regions other than the plateaux are attributed to the domain-wall (DW) phase and supersolid (SS), respectively. (b) Magnetic field dependence of the ultrasonic properties, the relative change in elastic constant $\Delta C_{66}/C_{66}$ (left axis) and its field derivative $d(\Delta C_{66}/C_{66})/dH$ (right axis) at 0.6 K. The red (blue) curve exhibits the data measured in the up (down) field sweep. The colored areas, determined by the dips of $d(\Delta C_{66}/C_{66})/dH$, correspond to the colors used in (a).

measured multiple single crystals using different measurement techniques and confirmed the consistency of the measured C_p values. A magnetocaloric effect (MCE) measurement was conducted in a pulsed field, which was generated by a long-pulse magnet for a long duration of 1.2 s. The ultrasonic properties of the sample, used for the MCE measurement, were also investigated using a conventional pulse-echo technique at 0.6 K. The in-plane transverse mode (C_{66} mode, wave vector $\mathbf{k} \parallel \mathbf{a}$, polarization vector $\mathbf{u} \parallel \mathbf{b}$) was measured using LiNbO_3 resonant transducers (X41° cut) at a frequency of 15 MHz. In this study, all the data were obtained by applying magnetic fields along the c axis.

First, as a guide to search for the intermediate phase, we present the ultrasonic properties of the magnetic Devil's staircase with the reported low-temperature magnetization [Fig. 2(a)] [13]. Figure 2(b) shows the relative change in the elastic constant $\Delta C_{66}/C_{66}$ in the up and down field sweeps (left axis) and the first field derivative $d(\Delta C_{66}/C_{66})/dH$ (right axis). Similar to the earlier report with a field parallel to the a axis [24], the data show a strong softening of C_{66} above 27 T, and there are several additional anomalies in the present data, most likely due to the differences in the field direction and temperature. Although the hysteresis depending on the field-sweep directions, which is most likely due to the first-order transitions and/or magnetocaloric effects, is observed, these field dependences in both sweeps are qualitatively identical. Some of the anomalies, probed by the minima of $d(\Delta C_{66}/C_{66})/dH$, are attributable to the previously reported phase boundaries of the

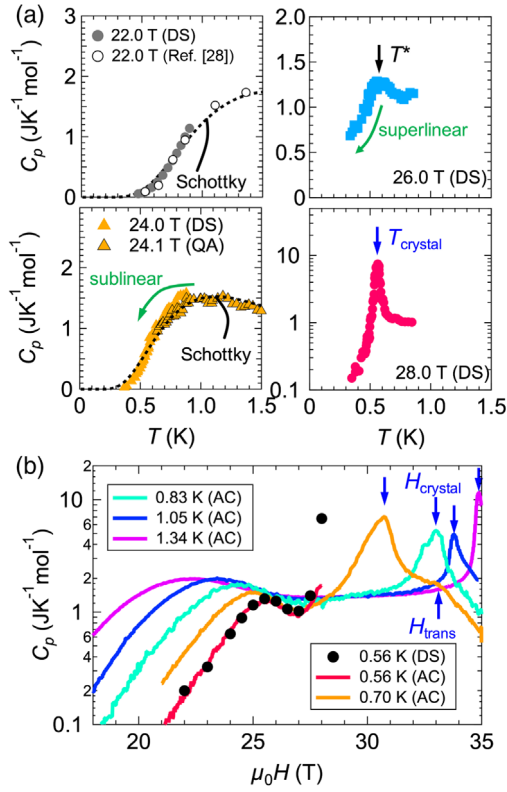


FIG. 3. (a) High-field C_p as a function of temperature. The data were measured by the dual-slope (DS) method and the quasi-adiabatic (QA) method. The 22.0 T data reported in Ref. [28] are also shown. The dotted curves obtained for 22.0 T and 24.0 T exhibit the Schottky behavior. Note that the data at 28.0 T are plotted on a semilogarithmic scale for clarity. (b) Magnetic field dependence of C_p measured by the ac (AC) method at various temperatures. For comparison, the dataset measured by the DS method at 0.56 K is also shown. The arrows indicate the anomalies in $C_p(H)$ curves caused by the crystallization and the transformation of the spin structure.

plateaux [13]. According to the theoretical prediction [17], some can be identified as the phase boundaries of the domain-wall (DW) states (light blue areas) predicted between the $2/15$ ($1/6$) and $1/6$ ($1/4$) plateaux, while the other anomalies are the phase boundaries of the supersolid (SS) state expected just below 34 T (purple area).

Figure 3(a) illustrates the temperature dependence of C_p at various fields (for complete datasets, see Supplemental Material [25]). The previously reported data for 22 T [28] are also shown for comparison. A sharp singularity is observed at $T = 0.55$ K and $H = 28$ T. Based on the phase diagram in Refs. [28–30], this large singularity corresponds to the transition to the $1/8$ -plateau phase. Remarkably, the height of the anomaly is several times larger than that of the first-order transition observed in the recent high-pressure experiment [20], and strongly suggests the first-order nature of the crystallization. Up to 24 T, the temperature dependence of $C_p(T)$ can be described by the Schottky-type

gapped behavior [see the dotted curve in Fig. 3(a)]. The Schottky anomaly exhibits a sublinear behavior around the maximum of the anomaly. It can be assumed that the spin gap between the singlet ground state and the excited state, Δ , vanishes with increasing magnetic field owing to the Zeeman energy. However, at 26 T, $C_p(T)$ deviates from the Schottky behavior, and a relatively sharp peak appears at $T^* \sim 0.6$ K with the superlinear temperature dependence just below T^* . The size of the C_p jump at T^* is about $0.2 \text{ JK}^{-1} \text{ mol}^{-1}$, which is comparable with those of the pressure-induced magnetic phase transitions (0.2 – $0.3 \text{ JK}^{-1} \text{ mol}^{-1}$) in $\text{SrCu}_2(\text{BO}_3)_2$ [10,20]. At 26 T, magnetic transitions have not been detected by any probes [11–15,29,30], and thus, the anomaly indicates the presence of a magnetically hidden state around 26 T. Moreover, the large C_p at temperatures lower than T^* indicates that the large entropy remains at low temperatures, suggesting the existence of low-energy collective excitations, namely, the Goldstone mode of the hidden order parameter. In Fig. 3(b), we present C_p measured by the AC method as a function of the magnetic field at each temperature to examine the C_p data from a different perspective. Above 30 T, each curve exhibits a large singularity at $H_{\text{crystal}}(T)$ originating from the crystallization of the multiplets, which has been detected by various magnetic probes. The small shoulder, which is denoted by H_{trans} , indicates the transformation of the spin structure between the DW and SS states [17]. The data below 28 T obtained by the DS method (black dot) agree with the data taken by the AC method. Below 24 T, the $C_p(H)$ data exhibit the Schottky-type broad bump that shifts its maximum towards higher temperature with the spin gap opening.

Figure 4(a) shows the field-temperature phase diagram deduced from the present (filled symbol) and previous studies (open symbols) [28–30]. The phase assignment is based on the theoretical prediction [17] and the magnetization data [13]. The obtained phase diagram below 33 T is in agreement with the previous studies. Additionally, we found that the slope of the phase boundary of H_{crystal} changes discontinuously at 33 T. According to the magnetic Clausius-Clapeyron equation, $dT_c/dH_c = -\Delta M/\Delta S$, this behavior is related to the large magnetization jump at 33–34 T [see Fig. 2(a)]. Notably, the theory [17] suggests that the crystals of the $S^z = 2$ bound triplets are energetically most favorable up to the $1/6$ plateau. However, for the $1/4$ plateau, the spin structure of the $S^z = 1$ is the same as that of the $S^z = 2$. This could be related to the kink in the (H, T) phase diagram. The hidden phase detected by our C_p data in the field region of 25–27 T has never been reported in previous studies. Below 25 T, it is hard to determine the lower-field phase boundary precisely.

For further identification of the phases from an entropic viewpoint, we present the results of the MCE under adiabatic conditions [Fig. 4(b)]. The data taken in the

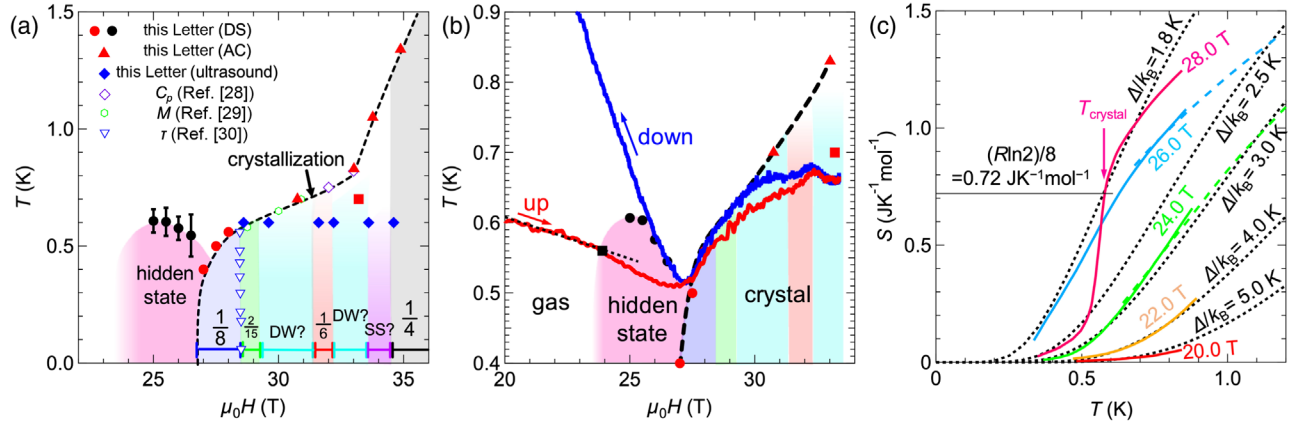


FIG. 4. (a) Temperature-field phase diagram of SrCu₂(BO₃)₂. The dashed curve is a visual guide to emphasize the crystal phase. The colors of the shaded areas correspond to those of the phases shown in Figs. 2(a) and 2(b). (b) Quasiadiabatic magnetocaloric effect in a pulsed magnetic field. The red (blue) curve represents the field-dependent temperature in the up-sweep (down-sweep). The dashed curve, the colored areas, and the symbols are the same as those shown in (a). The black square indicates the field where the MCE curve shows a kink. (c) Temperature dependence of entropy at each field. The black dotted lines represent the calculated curves of the Schottky-type entropy with the energy gap Δ/k_B . The dashed curves overlapping with the 24.0 T and 26.0 T data were derived from the data at 24.1 T and 26.2 T for the QA measurements. The thin black line indicates 0.72 J/Kmol , $(R \ln 2)/8$, which corresponds to the entropy of the $1/8$ plateau at T_{crystal} .

up-sweep and the down-sweep are plotted as red and blue curves, respectively. The data are qualitatively consistent with the reported quasi-isothermal MCE curve [14], even though the thermal condition in Ref. [14] was different from that in the present study. Moreover, we found that the MCE data during the field up-sweep show a kink around 24 T (black square), which can be attributed to the entrance of the hidden phase. This implies that the hidden state shows a dome-shaped phase diagram with a lower critical field of about 23–24 T, as shown by the pink area in Figs. 4(a) and 4(b). It should be noted that, below 27 T, the MCE curves show a large hysteresis between the up-sweep and down-sweep. The hysteresis in the gapped region may originate from the spin-glass-like slow dynamics observed in the μ SR study [31]. It can be interpreted that the magnetic disorder is frozen in the up-sweep; once the state undergoes crystallization above 27 T, the magnetic entropy can be released and the MCE exhibits a proper isentropic curve in the down-sweep. Therefore, based on the down-sweep MCE curve and the C_p data, we estimated the entropy S at various fields as a function of temperature, as shown in Fig. 4(c). The dotted curves represent the Schottky-type behavior with the shown Δ . As mentioned above, the datasets below 24 T are reproduced well by the Schottky behavior. However, the entropy data at 26 T shows the large entropy at low temperatures (< 0.5 K) and deviates from the Schottky behavior. It should be noted that, at 28 T, the entropy of the $1/8$ plateau reaches $(R \ln 2)/8$ at the crystallization temperature, T_{crystal} . This is because the number of triplets at the $1/8$ plateau is $N_A/8$ per mole, which is related to crystallization below T_{crystal} . The coincidence, $S = (R \ln 2)/N$ at T_{crystal} in a $1/N$ plateau, was observed in other plateau phases [32].

We now discuss the origin of the hidden state appearing on the ground floor of the magnetic Devil’s staircase. It should be emphasized that the NMR spectrum does not show any splitting below 26.5 T [12], indicating that the peak in C_p is not attributed to any order of magnetic dipoles. As noted earlier, in this field region, theoretical investigations predicted the SN order, namely, the condensation of the $S^z = 2$ bound triplets, which does not split the NMR spectrum. Experimentally, the peak at 26 T cannot be attributed to the soft mode of the $S^z = 1$ state, primarily because the ESR study [16] reports that the energy level of the $S^z = 2$ mode becomes lower than that of the $S^z = 1$ mode. Note that the ESR detects the signals of the $S^z = 1$ and 2 states at ~ 100 GHz around 20 T, whose energy scale is ~ 5 K, consistent with the value of Δ/k_B obtained in the present data [Figs. 1 and 4(c)]. Above 20 T, the $S^z = 2$ signal in the ESR spectrum is smeared out. However, a simple extrapolation of the low-field data yields a crossing field between the $S^z = 0$ and 2 states around $H^* = 24$ T. The H^* value is also confirmed by the $1/T_1$ experiment [33], where the spin gap is approximately 5 K at 20 T and becomes almost negligible around 24 T. Even if the energy levels are anticrossed around H^* , the characteristic of the ground state originates from the $S^z = 2$ bound triplets above H^* (see Supplemental Materials for further discussions [25]). The deviation of $C_p(T)$ above H^* from the Schottky behavior indicates that the anomaly at T^* results from the cooperative phenomenon of the macroscopically existing bound triplets. The contribution from the $S^z = 1$ state should be negligible because the energy gap between $S^z = 0$ and $S^z = 1$ is roughly 5 K even around 24 T [16], which only leads to small entropy below 1 K, as seen in the case of $\Delta/k_B = 5$ K in Fig. 4(c). Since the dispersive character of the $S^z = 2$ level [19] permits its

condensation, the requirement for the emergence of the SN order is satisfied in the field region showing the peak in C_p . The observed peak is relatively less significant than those of the typical phase transitions probably because of low dimensionality of $\text{SrCu}_2(\text{BO}_3)_2$. In most cases, the low dimensionality broadens the peak structure in C_p . Such broadened anomalies are observed for the pressure-induced magnetic orders in $\text{SrCu}_2(\text{BO}_3)_2$ [10,20].

Assuming that the hidden state is the SN order, two different SN orders, namely, plaquette SN and antiferro-SN orders, are predicted for $\text{SrCu}_2(\text{BO}_3)_2$ [21,22]. The structural difference between the two SNs is the order vector, \mathbf{k} . The antiferro-SN order with $\mathbf{k} = (\pi, \pi)$ breaks the C_4 lattice rotational symmetry and hosts the modulation of the magnetic dipole moment, whereas the plaquette SN order with $\mathbf{k} = (0, 0)$ possesses rotational symmetry locally even though the U(1) symmetry of global spin rotations is broken. In contrast to the antiferro-SN phase, the plaquette SN order shows no NMR spectrum splitting. Hence, the plaquette SN state is a more plausible candidate for the observed hidden state. Notably, the NMR relaxation rate [33] in the SN state is expected to be $1/T_1 \propto T^7$ [34,35]. Since the large power index is difficult to distinguish from the exponential behavior in the reported temperature region, the NMR data does not contradict our present results. The conclusion supports the theory [22] indicating that the plaquette SN order is the most favorable for the experimentally determined $J'/J = 0.60\text{--}0.64$ [8,14,36,37].

In summary, our high-field thermodynamic investigation demonstrates that $\text{SrCu}_2(\text{BO}_3)_2$ exhibits a magnetically hidden order around 26 T and various magnetic crystal states above 27 T. The hidden state is distinct from the lower-field gapped state; for example, $C_p(T)$ cannot be explained by the Schottky behavior. The large low-temperature heat capacity and entropy indicate the presence of low-energy excitations that originate from the dispersive $S^z = 2$ level. Based on the theoretical predictions, we interpret that the $S^z = 2$ bound triplets condense around 26 T and form the plaquette SN state. Further identification of this hidden state using other probes active to the spin quadrupole is a topic to be considered for future studies.

The authors would like to thank F. Mila, M. Takigawa, Z. Wang, and C. D. Batista for fruitful discussions and comments. This work was partially supported by JSPS KAKENHI Grants (20K14406, 20K14403, 22H04466, 22H00104), JSPS Core-to-Core Program (JPJSCCA20200004), UTEC-UTokyo FSI Research Grant Program, and by LNCMI-CNRS, member of the European Magnetic Field Laboratory (EMFL).

*imajo@issp.u-tokyo.ac.jp

†Present address: Research Institute for Interdisciplinary Science, Okayama University, Okayama 700-8530, Japan.

‡Present address: Department of Applied Chemistry, Ritsumeikan University, Kusatsu, Shiga 525-8577, Japan.

- [1] H. Kageyama, K. Yoshimura, R. Stern, N. V. Mushnikov, K. Onizuka, M. Kato, K. Kosuge, C. P. Slichter, T. Goto, and Y. Ueda, Exact Dimer Ground State and Quantized Magnetization Plateaus in the Two-Dimensional Spin System $\text{SrCu}_2(\text{BO}_3)_2$, *Phys. Rev. Lett.* **82**, 3168 (1999).
- [2] H. Kageyama, K. Onizuka, T. Yamauchi, and Y. Ueda, Crystal growth of the two-dimensional spin gap system $\text{SrCu}_2(\text{BO}_3)_2$, *J. Cryst. Growth* **206**, 65 (1999).
- [3] B. S. Shastry and B. Sutherland, Exact ground state of a quantum mechanical antiferromagnet, *Physica (Amsterdam)* **108B**, 1069 (1981).
- [4] S. Miyahara and K. Ueda, Exact Dimer Ground State of the Two Dimensional Heisenberg Spin System $\text{SrCu}_2(\text{BO}_3)_2$, *Phys. Rev. Lett.* **82**, 3701 (1999).
- [5] A. Koga and N. Kawakami, Quantum Phase Transitions in the Shastry-Sutherland Model for $\text{SrCu}_2(\text{BO}_3)_2$, *Phys. Rev. Lett.* **84**, 4461 (2000).
- [6] T. Waki, K. Arai, M. Takigawa, Y. Saiga, Y. Uwatoko, H. Kageyama, and Y. Ueda, A novel ordered phase in $\text{SrCu}_2(\text{BO}_3)_2$ under high pressure, *J. Phys. Soc. Jpn.* **76**, 073710 (2007).
- [7] M. E. Zayed *et al.*, 4-spin plaquette singlet state in the Shastry-Sutherland compound $\text{SrCu}_2(\text{BO}_3)_2$, *Nat. Phys.* **13**, 962 (2017).
- [8] T. Sakurai, Y. Hirao, K. Hijii, S. Okubo, H. Ohta, Y. Uwatoko, K. Kudo, and Y. Koike, Direct observation of the quantum phase transition of $\text{SrCu}_2(\text{BO}_3)_2$ by high-pressure and terahertz electron spin resonance, *J. Phys. Soc. Jpn.* **87**, 033701 (2018).
- [9] C. Boos, S. P. G. Crone, I. A. Niesen, P. Corboz, K. P. Schmidt, and F. Mila, Competition between intermediate plaquette phases in $\text{SrCu}_2(\text{BO}_3)_2$ under pressure, *Phys. Rev. B* **100**, 140413(R) (2019).
- [10] J. Guo, G. Sun, B. Zhao, L. Wang, W. Hong, V. A. Sidorov, N. Ma, Q. Wu, S. Li, Z. Y. Meng, A. W. Sandvik, and L. Sun, Quantum Phases of $\text{SrCu}_2(\text{BO}_3)_2$ from High-Pressure Thermodynamics, *Phys. Rev. Lett.* **124**, 206602 (2020).
- [11] K. Onizuka, H. Kageyama, Y. Narumi, K. Kindo, Y. Ueda, and T. Goto, 1/3 magnetization plateau in $\text{SrCu}_2(\text{BO}_3)_2$ -stripe order of excited triplets-, *J. Phys. Soc. Jpn.* **69**, 1016 (2000).
- [12] K. Kodama, M. Takigawa, M. Horvatić, C. Berthier, H. Kageyama, Y. Ueda, S. Miyahara, F. Becca, and F. Mila, Magnetic superstructure in the two-dimensional quantum antiferromagnet $\text{SrCu}_2(\text{BO}_3)_2$, *Science* **298**, 395 (2002).
- [13] M. Takigawa, M. Horvatić, T. Waki, S. Krämer, C. Berthier, F. Lévy-Bertrand, I. Sheikin, H. Kageyama, Y. Ueda, and F. Mila, Incomplete Devil's Staircase in the Magnetization Curve of $\text{SrCu}_2(\text{BO}_3)_2$, *Phys. Rev. Lett.* **110**, 067210 (2013).
- [14] M. Jaime, R. Daou, S. A. Crooker, F. Weickert, A. Uchida, A. E. Feiguin, C. D. Batista, H. A. Dabkowska, and B. D. Gaulin, Magnetostriction and magnetic texture to 100.75 Tesla in frustrated $\text{SrCu}_2(\text{BO}_3)_2$, *Proc. Natl. Acad. Sci. U.S.A.* **109**, 12404 (2012).

- [15] S. Haravifard, D. Graf, A. E. Feiguin, C. D. Batista, J. C. Lang, D. M. Silevitch, G. Srajer, B. D. Gaulin, H. A. Dabkowska, and T. F. Rosenbaum, Crystallization of spin superlattices with pressure and field in the layered magnet $\text{SrCu}_2(\text{BO}_3)_2$, *Nat. Commun.* **7**, 11956 (2016).
- [16] H. Nojiri, H. Kageyama, Y. Ueda, and M. Motokawa, ESR study on the excited state energy spectrum of $\text{SrCu}_2(\text{BO}_3)_2$ —A central role of multiple-triplet bound states—, *J. Phys. Soc. Jpn.* **72**, 3243 (2003).
- [17] P. Corboz and F. Mila, Crystals of Bound States in the Magnetization Plateaus of the Shastry-Sutherland Model, *Phys. Rev. Lett.* **112**, 147203 (2014).
- [18] T. Momoi and K. Totsuka, Magnetization plateaus of the Shastry-Sutherland model for $\text{SrCu}_2(\text{BO}_3)_2$: Spin-density wave, supersolid, and bound states, *Phys. Rev. B* **62**, 15067 (2000).
- [19] H. Kageyama, M. Nishi, N. Aso, K. Onizuka, T. Yoshida, K. Nukui, K. Kodama, K. Kakurai, and Y. Ueda, Direct Evidence for the Localized Single-Triplet Excitations and the Dispersive Multitriplet Excitations in $\text{SrCu}_2(\text{BO}_3)_2$, *Phys. Rev. Lett.* **84**, 5876 (2000).
- [20] J. Larrea Jiménez, S. P. G. Crone, E. Fogh, M. E. Zayed, R. Lortz, E. Pomjakushina, K. Conder, A. M. Läuchli, L. Weber, S. Wessel, A. Honecker, B. Normad, Ch. Rüegg, P. Corboz, H. M. Rønnow, and F. Mila, A quantum magnetic analogue to the critical point of water, *Nature (London)* **592**, 370 (2021).
- [21] S. C. Furuya and T. Momoi, Electron spin resonance for the detection of long-range spin nematic order, *Phys. Rev. B* **97**, 104411 (2018).
- [22] Z. Wang and C. D. Batista, Dynamics and Instabilities of the Shastry-Sutherland Model, *Phys. Rev. Lett.* **120**, 247201 (2018).
- [23] S. Imajo, C. Dong, A. Matsuo, K. Kindo, and Y. Kohama, High-resolution calorimetry in pulsed magnetic fields, *Rev. Sci. Instrum.* **92**, 043901 (2021).
- [24] B. Wolf, S. Zherlitsyn, S. Schmidt, B. Lüthi, H. Kageyama, and Y. Ueda, Soft Acoustic Modes in the Two-Dimensional Spin System $\text{SrCu}_2(\text{BO}_3)_2$, *Phys. Rev. Lett.* **86**, 4847 (2001).
- [25] See Supplemental Material at <http://link.aps.org/supplemental/10.1103/PhysRevLett.129.147201> for the full dataset of the high-field heat capacity data and other information, which includes Refs. [16,18,19,22,26–28].
- [26] N. Shannon, T. Momoi, and P. Sindzingre, Nematic Order in Square Lattice Frustrated Ferromagnets, *Phys. Rev. Lett.* **96**, 027213 (2006).
- [27] G. Misguich and M. Oshikawa, Bose-Einstein condensation of magnons in TlCuCl_3 : Phase diagram and specific heat from a self-consistent Hartree-Fock calculation with a realistic dispersion relation, *J. Phys. Soc. Jpn.* **73**, 3429 (2004).
- [28] H. Tsujii, C. R. Rotundu, B. Andraka, Y. Takano, H. Kageyama, and Y. Ueda, Specific heat of the $S=1/2$ two-dimensional Shastry-Sutherland antiferromagnet $\text{SrCu}_2(\text{BO}_3)_2$ in high magnetic field, *J. Phys. Soc. Jpn.* **80**, 043707 (2011).
- [29] M. Takigawa, S. Matsubara, M. Horvatić, C. Berthier, H. Kageyama, and Y. Ueda, NMR Evidence for the Persistence of a Spin Superlattice Beyond the $1/8$ Magnetization Plateau in $\text{SrCu}_2(\text{BO}_3)_2$, *Phys. Rev. Lett.* **101**, 037202 (2008).
- [30] F. Levy, I. Sheikin, C. Berthier, and M. Horvatić, M. Takigawa, H. Kageyama, T. Waki, and Y. Ueda, Field dependence of the quantum ground state in the Shastry-Sutherland system $\text{SrCu}_2(\text{BO}_3)_2$, *Europhys. Lett.* **81**, 67004 (2008).
- [31] Y. Sassa, S. Wang, J. Sugiyama, A. Amato, H. M. Rønnow, C. Rüegg, and M. Månsson, μ^+ SR investigation of the Shastry-Sutherland compound $\text{SrCu}_2(\text{BO}_3)_2$, *J. Phys. Soc. Jpn. Conf. Proc.* **21**, 011010 (2018).
- [32] S. Akimoto and Y. H. Matsuda (private communication).
- [33] K. Kodama, S. Miyahara, M. Takigawa, M. Horvatić, C. Berthier, F. Mila, H. Kageyama, and Y. Ueda, Field-induced effects of anisotropic magnetic interactions in $\text{SrCu}_2(\text{BO}_3)_2$, *J. Phys. Condens. Matter* **17**, L61 (2005).
- [34] A. Smerald and N. Shannon, Theory of NMR $1/T_1$ relaxation in a quantum spin nematic in an applied magnetic field, *Phys. Rev. B* **93**, 184419 (2016).
- [35] R. Shindou, S. Yunoki, and T. Momoi, Dynamical spin structure factors of quantum spin nematic states, *Phys. Rev. B* **87**, 054429 (2013).
- [36] C. Knetter, A. Bühler, E. Müller-Hartmann, and G. S. Uhrig, Dispersion and Symmetry of Bound States in the Shastry-Sutherland Model, *Phys. Rev. Lett.* **85**, 3958 (2000).
- [37] Y. H. Matsuda, N. Abe, S. Takeyama, H. Kageyama, P. Corboz, A. Honecker, S. R. Manmana, G. R. Foltin, K. P. Schmidt, and F. Mila, Magnetization of $\text{SrCu}_2(\text{BO}_3)_2$ in Ultrahigh Magnetic Fields up to 118 T, *Phys. Rev. Lett.* **111**, 137204 (2013).